ORIGINAL PAPER

Multiple Pathways Analysis of Brain Functional Networks from EEG Signals: An Application to Real Data

Fabrizio De Vico Fallani · Francisco Aparecido Rodrigues ·
Luciano da Fontoura Costa · Laura Astolfi · Febo Cincotti ·
Donatella Mattia · Serenella Salinari · Fabio Babiloni

Abstract In the present study, we propose a theoretical graph procedure to investigate multiple pathways in brain functional networks. By taking into account all the possible paths consisting of h links between the nodes pairs of the network, we measured the global network redundancy R_h as the number of parallel paths and the global network permeability P_h as the probability to get connected. We used this procedure to investigate the structural and dynamical changes in the cortical networks estimated from a dataset of high-resolution EEG signals in a group of spinal cord injured (SCI) patients during the attempt of foot movement. In the light of a statistical contrast with a healthy population, the permeability index P_h of the SCI networks increased significantly ($P < 0.01$) in the Theta frequency band (3–6 Hz) for distances h ranging from 2 to 4. On the contrary, no significant differences were found between the two populations for the redundancy index R_h. The most significant changes in the brain functional network of SCI patients occurred mainly in the lower spectral contents. These changes were related to an improved propagation of communication between the closest cortical areas rather than to a different level of redundancy. This evidence strengthens the hypothesis of the need for a higher functional interaction among the closest *ROIs* as a mechanism to compensate the lack of feedback from the peripheral nerves to the sensomotor areas.

Keywords Cortical networks · Graph theory · Redundancy · Permeability · Spinal cord injury

F. De Vico Fallani (✉) · L. Astolfi · F. Cincotti · D. Mattia ·
F. Babiloni
Laboratory of Clinical Neurophysiopathology, IRCCS
"Fondazione Santa Lucia", Via Ardeatina, 306, I-00179 Rome,
Italy
e-mail: fabrizio.devicofallani@uniroma1.it

F. De Vico Fallani · F. Babiloni
Department of Human Physiology and Pharmacology,
University "Sapienza", Rome, Italy

F. A. Rodrigues
Departamento de Matemática Aplicada e Estatística, Instituto de
Ciências Matemáticas e de Computação, Universidade de São
Paulo, São Paulo, Brazil

L. Astolfi · S. Salinari
Department of Informatica e Sistemistica, University
"Sapienza", Rome, Italy

L. da Fontoura Costa
Instituto de Física de São Carlos, Universidade de São Paulo,
São Paulo, Brazil

Introduction

Over the last years, a growing interest has focused on the development and validation of computational tools for the analysis of complex brain networks (Sporns 2002; Stam 2004; Tononi et al. 1994). Since a graph is a mathematical representation of a network, which is essentially reduced to nodes and connections between nodes, the use of a graph-theoretical approach has been found potentially relevant and useful, as first demonstrated on a set of anatomical brain networks (Sporns et al. 2000; Stephan et al. 2000; Strogatz 2001). In those studies, the authors employed two characteristic features, the average shortest path L and the clustering coefficient C, in order to extract, respectively, the global and local properties of the network structure. They found that anatomical brain networks exhibit many local connections—i.e,. a high C—and few random long distance connections—i.e., a low L-characterizing a particular model that interpolate between a regular lattice and

a random structure (Watts and Strogatz 1998). Such a model has been designated as the "small-world" network in analogy with the concept of the small-world phenomenon observed more than 30 years ago in social systems (Milgram 1967). Subsequently, many types of functional brain networks have been analyzed according to this mathematical approach. In particular, several studies-based on different imaging techniques like *fMRI* (Salvador et al. 2005; Eguiluz et al. 2005; Achard and Bullmore 2007), MEG (Bassett et al. 2006; Bartolomei et al. 2006; Stam et al. 2006; Chavez et al. 2010) and EEG (Micheloyannis et al. 2006; Stam et al. 2007; Ponten et al. 2007; De Vico Fallani et al. 2008)—have found that the estimated functional networks also exhibit small-world characteristics. Such a topological property of the network has a strong impact on neurosciences, since it is related to optimal architectures for information processing and signal transmission between different cerebral structures (Lago-Fernandez et al. 2000; Sporns et al. 2004; Bullmore and Sporns 2009). The small-world concept in complex networks is closely related to the length of the shortest paths, which is given by the smallest number of connections that are needed to go from a starting vertex i to a target node j (Watts and Strogatz 1998). However, shortest paths just represent one possible way in which two nodes in a graph can communicate. Existing longer pathways should be generally taken into account when characterizing a connectivity pattern. Recently, a novel method—called superedges—founded on the evaluation of multiple paths between network elements has been proposed in the literature (Costa and Rodriguez 2008). From a neuroscientific perspective, the possibility to inspect multiple parallel pathways seems closely related to a concept of redundancy and robustness, which is supposed to be a natural mechanism of the brain for enhancing the resilience to neural damages and dysfunctions (Rossini 2000). In the present study, we introduce two graph indexes based on the superedges method to extract the redundancy R_h—the average number of alternative paths between all the node pairs-and the permeability P_h—the average probability to get connected between all the node pairs-of a network for a given path length h. In order to evaluate the potential of the proposed approach we consider a dataset of brain functional networks which has been studied previously through the standard small-world analysis (De Vico Fallani et al. 2007). In that work, cortical networks have been obtained from a set of high-resolution EEG signals in a group of spinal cord injured patients and control subjects during the preparation of an intended motor act.

The aim of the present study is to provide a more complete description of the possible structural and dynamical changes in the cortical networks of the spinal cord injured patients through a multiple pathways analysis.

Methods

The experimental subjects participating in the study were recruited by advertisement. Informed consent was obtained in each subject after the explanation of the study, which was approved by the local institutional ethics committee. The spinal cord injured group (SCI) consisted of five patients (age, 22–25 years; two females and three males). Spinal cord lesions were of traumatic etiology and located at the cervical level (C6 in three cases, C5 and C7 in two cases, respectively). The control group (CTRL) included five healthy volunteers (age, 26–32 years; five males). For the EEG data acquisition, the experimental subjects were comfortably seated on a reclining chair, in an electrically shielded and dimly lit room. The experimental task for the SCI patients consisted in the performance of a brisk protrusion of their lips at the same time as they attempted (volition task) to move their right foot. The same task was performed by the CTRL subjects except to the fact that they executed really the foot movement. The choice of this combined task was suggested by the possibility to trigger the patients' attempt of foot movement by an electromyographic (EMG) signal recorded from their lips. The task was repeated every 8 s in a self-paced manner and 100 single trials were recorded. A 96-channel system (Brain-Amp, Brainproducts GmbH, Germany) was used to record simultaneously the 64 EEG signals from the scalp and the EMG signals from the lips. The frequency sampling was 200 Hz. Afterwards, the EEG signals were inspected for artifacts rejection and band-pass filtered (1–50 Hz). Before the experiment, structural MRI images of the head of each experimental subject were acquired by means of a Siemens 1.5 T Vision Magnetom MR system (Germany), in order to model the head tissues separating the cortex from the scalp.

Functional Connectivity from High-Resolution EEG

Cortical activity was obtained from 64 scalp EEG signals by using a technique known as high-resolution EEG (Le and Gevins 1993; Gevins et al. 1994; Babiloni et al. 2000). Such technology includes (i) the sampling of the spatial distribution of scalp potential with a larger number of surface electrodes (typically 64–256); (ii) the use of sequential magnetic resonance images (MRI) to describe mathematically the different conductivity effects of the inner head structures between scalp and cortex; (iii) the solution to a linear inverse problem to estimate the original EEG signals generated in the cortex from the measured scalp signals. By using the passage through the Tailairach coordinates system, 12 regions of interest (*ROIs*) were then obtained by the segmentation of Brodmann areas on each accurate cortical model consisting of about 5,000 electrical dipoles, i.e., the cortical sources. The considered *ROIs* are

particularly involved in the cerebral processing of the foot-lips movement (Mattia et al. 2009). They are the primary motor areas of the foot in the left (MF_L) and right (MF_R) hemisphere; the primary motor areas of the lip (ML_L and ML_R); the proper supplementary motor areas (SM_L and SM_R); the global pre-motor areas (6_L and 6_R); the cingulate motor areas (CM_L and CM_R) and the associative parietal areas (7_L and 7_R). The temporal signals in the *ROIs* were finally obtained by averaging the signals of the dipoles within the corresponding segmented areas. Such time-series just represent the instantaneous current density in the 12 regions of interest. It means that from 64 scalp electrode time-series, we are able to estimate 12 cortical time-series representing the "real" activity of the cortex throughout the preparation of the movement. In particular, a temporal segment of 1.5 s before the lips pursing—i.e., the event trigger-was considered to study the cerebral behavior during the movement preparation, which is able to reveal the first changes in the electrical activity (event related desynchronization—ERD, Pfurtsheller and Lopes da Silva 1999). This particular time segment also avoided that muscular artifacts due to the lips movement execution could affect the EEG signals.

The resulting cortical waveforms were simultaneously processed for the functional connectivity estimation by using the directed transfer function (DTF). The DTF is an estimator that simultaneously characterizes the direction and spectral properties of the interaction between brain signals and requires only one multivariate autoregressive (MVAR) model to be estimated simultaneously from all the time series (Kaminski et al. 2001). The advantages of MVAR modeling of multichannel EEG signals in order to compute efficient connectivity estimates have recently been stressed. Kus et al. (2004) demonstrated the superiority of MVAR multichannel modeling with respect to the pair-wise autoregressive approach. The DTF can be demonstrated (Kaminski et al. 2001) to rely on the key concept of Granger causality between time series (Granger 1969).

Granger theory mathematically defines what a "causal" relation between two signals is. According to this theory, an observed time series *x(n)* is said to cause another series *y(n)* if the knowledge of *x(n)*'s past significantly improves prediction of *y(n)*; this relation between time series is not necessarily reciprocal, i.e., *x(n)* may cause *y(n)* without *y(n)* causing *x(n)*. This lack of reciprocity allows the evaluation of the direction of information flow between structures. The equations used for the application of the DTF to EEG data are described fully in previous papers (Astolfi et al. 2006, 2007). By considering twelve *ROIs* the DTF yields a cortical network of twelve nodes for each standard frequency band of interest: Theta 4–7 Hz, Alpha 8–12 Hz, Beta 13–29 Hz, Gamma 30–40 Hz. Finally, only those functional connections that resulted statistically

significant ($P < 0.001$) after the contrast with a surrogate distribution of DTF values obtained from a Montecarlo procedure—were considered.

Cortical Network Analysis

A graph consists of a set of vertices (or nodes) and a set of edges (or connections) indicating the presence of some sort of interaction between the vertices. The adjacency matrix A contains the information about the connectivity structure of the graph. When a directed edge exists from the node i to j, the corresponding entry of the adjacency matrix is $A_{ij} = 1$; otherwise $A_{ij} = 0$. In graph theory, a path–or a walk–is a sequence of vertices such that from each of its vertices there is an edge to the next vertex in the sequence.

In the present work, all the estimated functional networks have the same number of unweighted links representing the 30%—i.e., 0.3 of connection density—most powerful links in the connectivity pattern. This particular value was comprised in an interval of threshold densities—from 0.1 to 0.5 for which results, obtained with a standard small-world analysis, remained significantly stable (De Vico Fallani et al. 2007). Here, we wanted to analyze the same dataset with the novel methodology, i.e. the multiple pathways. For this reason, we considered the same cortical networks in order to make a direct comparison between the small-world analysis (only shortest distance paths) and the present one (multiple distance paths). Figure 1 shows the brain functional networks estimated from a single representative *SCI* patient in the four characteristic ranges of EEG oscillations; while Fig. 2 shows the brain functional networks estimated from a single representative CTRL subject in the same frequency bands.

Network Structure

The most intuitive index to measure the redundancy level in the network structure is the number of walks between all the node pairs. These paths represent alternative routes of communication between the input and output elements. The number of paths with length h of a node i, $R_h(i)$, is given by the total number of paths of length h between that node and all the other nodes in the network:

$$R_h(i) = \sum_{j=1}^{N} r_h(i,j) \tag{1}$$

where $R_h(i,j)$ is the number of paths of length h starting at i reaching the vertex j. When a vertex i concentrates many alternative walks to another vertex j this implies that the communication between such vertices presents a high level of resilience against edge disruption. In fact, when an edge belonging to any of the paths between i and j is removed,
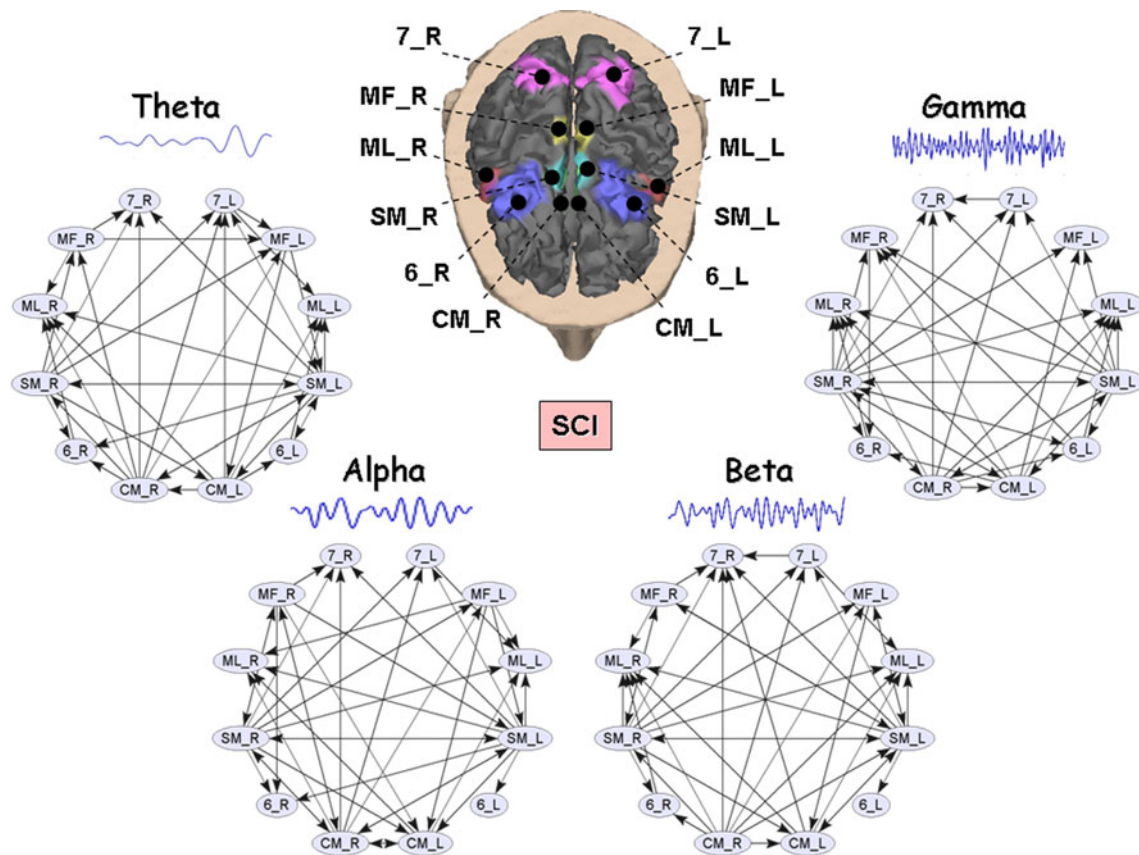
Fig. 1 Cortical networks estimated from the high-resolution EEG signals in a representative SCI patient during the movement preparation. Functional relationships between *ROIs* were evaluated in four main frequency bands, Theta (3–6 Hz), Alpha (7–12 Hz), Beta (13–29 Hz) and Gamma (30–40 Hz). Networks are represented as graphs. Each node corresponds to a particular *ROI*, which is highlighted in color on the actual cortex model. Each directed edge corresponds to a significant causal relationship between the electrical activities of two *ROIs*

the connection between these vertices are not interrupted. The average of all the $R_h(i)$ values gives a global measure of network redundancy for each distance h:

$$R_h = \frac{1}{N}\sum_{i=1}^{N} R_h(i) \tag{2}$$

$h \in [0, N-1]$, where N is the number of nodes. The higher is R_h the higher is the presence of multiple pathways of length h in the network.

Network Dynamics

A very interesting index to inspect the network dynamics can be quantified by considering the transition probability $P_h(i,j)$ between pair of nodes, which measures the probability of a self avoiding random walk starting from a vertex i to reach a vertex j after h steps. In other words, the transition probability—also known as "activation" between nodes (Rodrigues and Costa 2009)—measures the probability of two nodes to be connected. The activation of length h of a node i to all the other nodes is given by:

$$P_h(i) = \sum_{j=1}^{N} p_h(i,j) \tag{3}$$

If a vertex i has a high activation at distance h, then it is connected to a small number of "dead-ends" nodes that are distant h at least. Dead-ends nodes are those vertices where the path cannot propagate, which reduces the total activation. Figure 3 illustrates an example of four possible paths of different length between an input and output node of a directed graph. Panel c) shows a situation where the walk reaches a dead-end node. The average of all the $P_h(i)$ values gives a global measure of network permeability for each distance h:

$$P_h = \frac{1}{N}\sum_{i=1}^{N} P_h(i) \tag{4}$$

$h \in [0, N-1]$, where N is the number of nodes. Since the activation reflects a probability then $P_h \in [0, 1]$. The higher is P_h the higher is the tendency of the network to facilitate the diffusion and spreading of information. It is worth to observe that the outward activation is different from the concept of "network load" (Goh et al. 2001), which is based on the
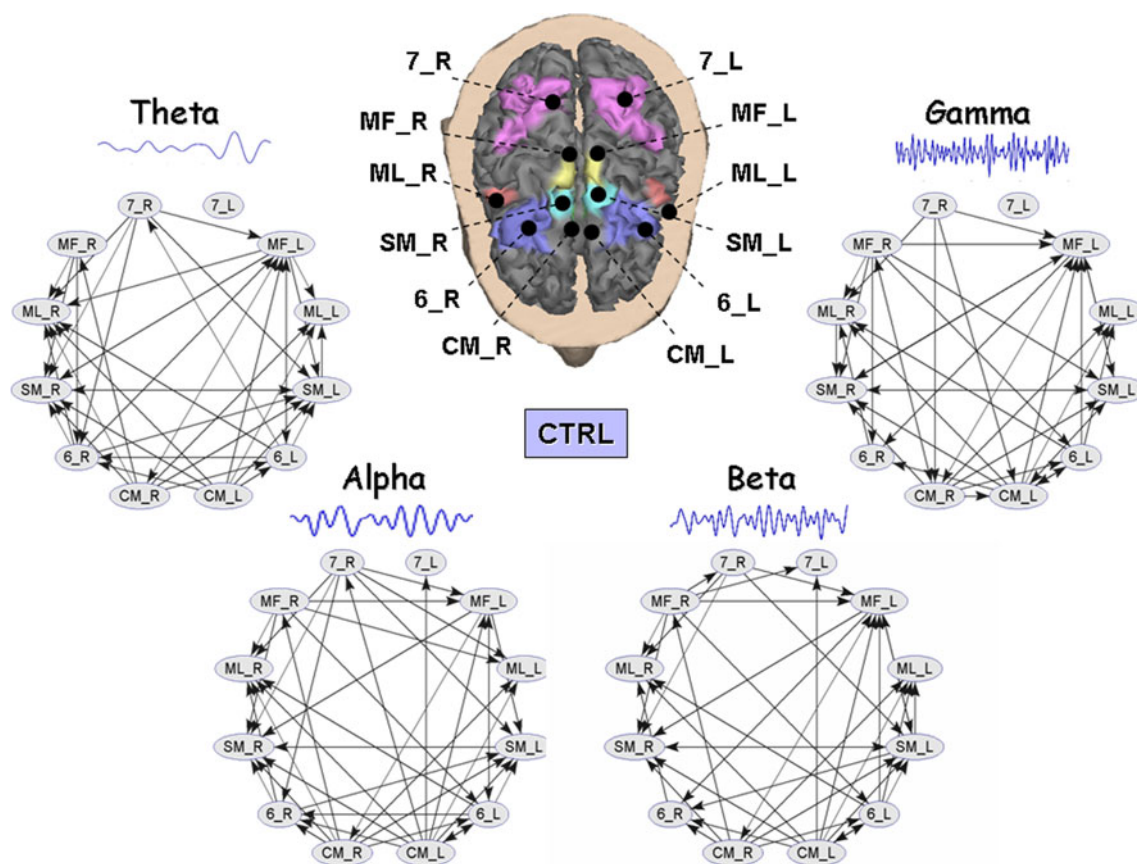
Fig. 2 Cortical networks estimated from the high-resolution EEG signals in a representative CTRL subject during the movement preparation. Same conventions as in Fig. 1

betweenness centrality measurement. In fact, a link with a high activation value propagates its influence across long distances (there are a few dead-ends in the paths of length h), while a link with a high "load", or betweenness centrality, is rather a specific link separating two communities.

Analysis of Variance

In order to catch inter-individual variance between subjects and within different path lengths we used the analysis of variance (ANOVA), separately for each graph index and frequency band. The main factors of the ANOVAs were the "between" factor GROUP with two levels, SCI and CTRL, and the "within" factor H—i.e., the distance or path length—with eight levels, from 2 to 9. Subsequently, a post-hoc analysis with the Duncan's test was performed to extract the eventual significant combinations between the independent factors.

Random Network Comparison

In order to have a means of contrast for the graph indexes evaluated in the cortical networks we computed the same

measures in a set of reference graphs whose links were arranged in a random fashion. In particular, one-hundred random graphs were generated by maintaining the same number of nodes and connections of the original cortical networks. Each time, links were shuffled in a random fashion without preserving the node degree distribution. The preservation of the degree distribution in the randomization process of large networks has been already demonstrated to generate a more robust comparison (Maslov and Sneppen 2002). However, in the present study the small size of the original cortical networks would not allow to produce such an advance as the small number of possible link permutations produces only similar connectivity patterns, this fact leading to non-significant contrasts.

Results

In the present study, the cortical network analysis was evaluated by considering path lengths ranging from 2 to 9 ($h = 2\ldots9$), where $h = 9$ is the maximum distance observed for all the networks. Distances $h = 1$ were neglected as the cortical networks held the same number of
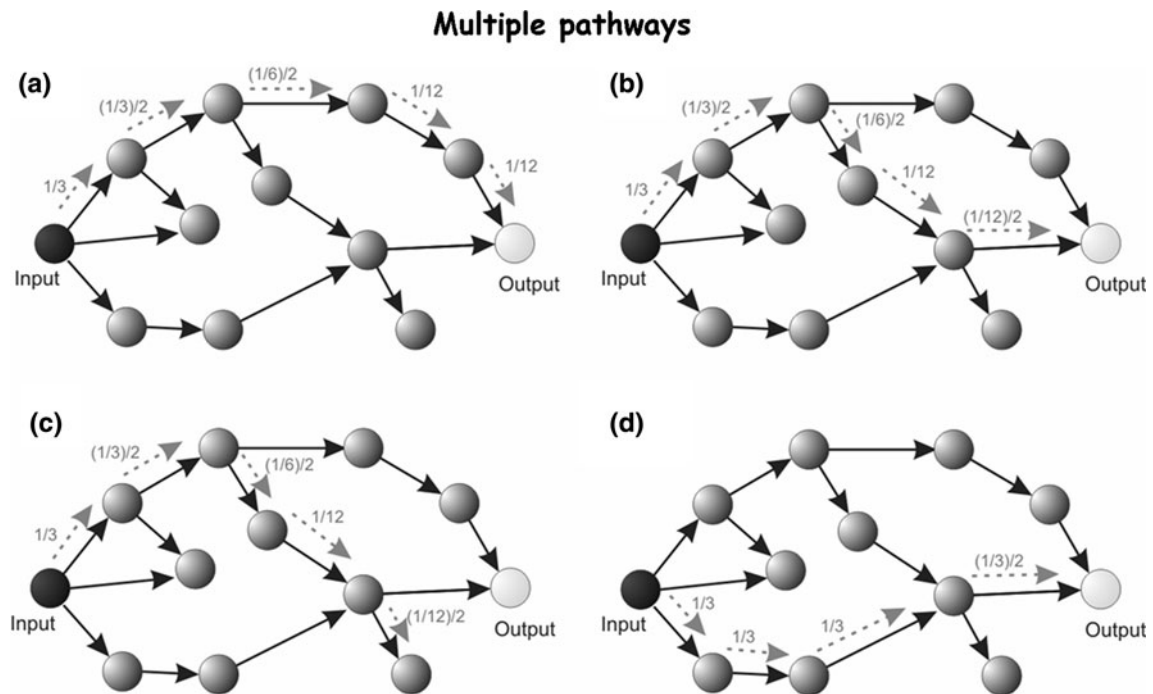
Multiple pathways

Fig. 3 Example of multiple pathways analysis. The same graph is represented in each panel, where dotted arrows indicate a possible self-avoiding random walk. At panel **a** the transition probability between two particular input and output nodes is 1/12. The probability at the first step is calculated by dividing one by the number of connections of the input (1/3). At each subsequent step, the transition probability is obtained by dividing the current probability by the number of non-visited vertices. At panel **b** the transition probability is 1/24. At panel **c** the particular walk does not reach the output. In this situation, the last reached node is called dead-end, i.e., a point of no continuation for the walk. At the panel **d** the transition probability is 1/6

connections and the presence of multiple pathways of length 1 in the network (R_1) was just equal to the connection density (the ratio of the actual number of links and the total number of possible links) of each network.

Network Redundancy

Figure 4 illustrates the mean R_h values in all the frequency bands calculated from the networks of the SCI patients and CTRL subjects. In general, the bell-shaped profiles of both the groups indicate the presence of a high number of alternative pathways at a medium-range connectivity (i.e., $h = 4,5,6$) and a lower parallel routes at the short-range ($h < 4$) and large-range ($h > 6$) connectivity. This characteristic behavior is confirmed statistically by the ANOVA effects of the "within" main factor H, which exhibited significant ($P < 0.01$) values in all the frequency bands (see Table 1).

Even if the mean values of the SCI networks are generally higher with respect to the CTRL networks in all the frequency bands but Gamma, their general profiles are not very separated.

In particular, the analysis of variance of the redundancy indexes for each separate frequency bands revealed no significant differences between the two analyzed populations (see main factor GROUP at Table 1).

The interaction effect GROUP x H is also not significant in all the frequency bands, preventing for any assessment of statistical difference between the two populations at particular connectivity ranges.

The mean R_h values obtained from random graphs can be observed at the top of Fig. 6. At any distance h, the mean redundancy values are significantly higher than those obtained either from CTRL and SCI subjects. Moreover, the observed profile clearly suggests the presence of a high number of alternative pathways at the largest-range connectivity (i.e., $h > 6$).

Network Permeability

Figure 5 illustrates the mean P_h values in all the frequency bands calculated from the networks of the SCI patients and CTRL subjects. In general, the decreasing profiles of both the groups indicate a high tendency of the cortical network to walk along the shortest paths ($h < 4$) and a low probability to cover the longest paths ($h > 7$).

This characteristic behavior is confirmed statistically by the ANOVA effects of the "within" main factor H, which exhibited significant ($P < 0.01$) values in all the frequency bands (see Table 2).

While no significant differences were observed between the two groups in the Alpha, Beta and Gamma band, a

Fig. 4 Profiles of the redundancy index R_h in all the frequency bands. The different path lengths h are shown on the x-axis. Blue circles represent mean values from the *SCI* group; red squares stand for the mean values from the *CTRL* group. Vertical bars indicate the respective standard deviation
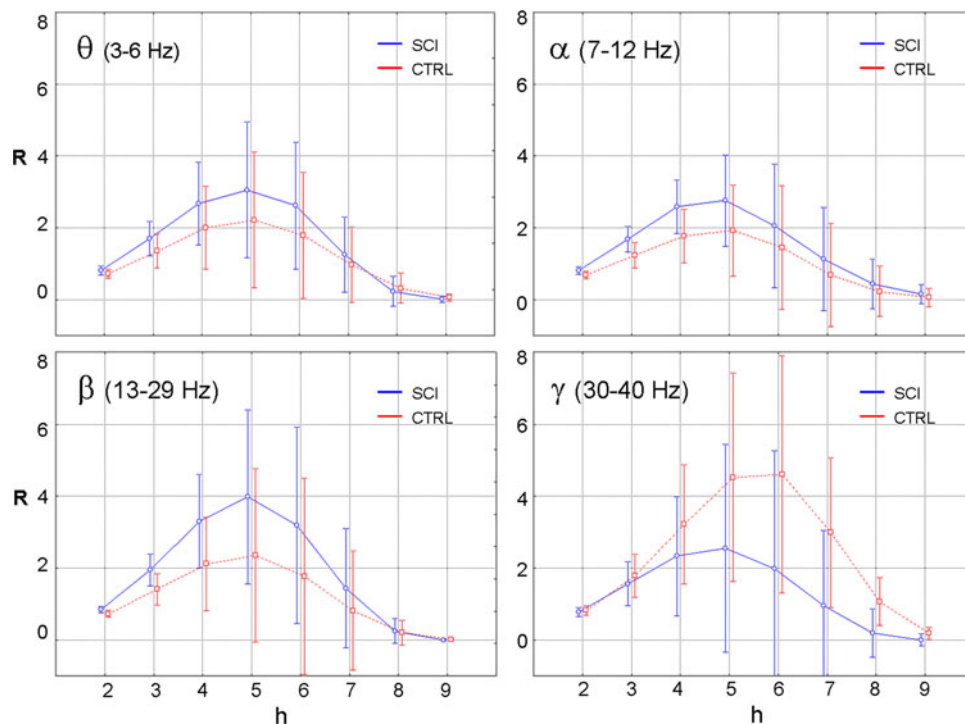

Table 1 ANOVA results of the redundancy index R_h for each frequency band

Distance *Band*	GROUP	H	GROUP *x H*
Theta	$F(1,8) = 0.517\ P = 0.52$	$F(7,56) = 17.544\ P < 0.001*$	$F(7,56) = 0.648\ P = 0.714$
Alpha	$F(1,8) = 0.934\ P = 0.362$	$F(7,56) = 17.393\ P < 0.001*$	$F(5,56) = 0.524\ P = 0.853$
Beta	$F(1,8) = 1.057\ P = 0.334$	$F(7,56) = 12.360\ P < 0.001*$	$F(7,56) = 0.928\ P = 0.493$
Gamma	$F(1,8) = 1.671\ P = 0.233$	$F(7,56) = 11.621\ P < 0.001*$	$F(7,56) = 1.567\ P = 0.167$

The asterisk symbol * indicates the values $P < 0.01$

significant ($P < 0.01$) effect was found in the Theta band for the main factor GROUP and for the interaction factor GROUP x H, too (see Table 2). In particular, the post-hoc test revealed a significant higher P_h value of the SCI group with respect to the CTRL group at the first distances $h = 2$ ($P = 0.00102$), $h = 3$ ($P = 0.00006$), $h = 4$ ($P = 0.00004$), $h = 5$ ($P = 0.00145$).

The mean P_h values obtained from random graphs can be observed at the bottom of Fig. 6. At any distance h, the mean permeability values are significantly higher than those obtained either from CTRL and SCI subjects. As for the cortical networks, the decreasing profiles indicate a high tendency of the random pattern to walk along the shortest paths ($h < 4$) and a low probability to cover the longest paths ($h > 7$).

Discussion

The solely consideration of shortest path distances could provide an incomplete characterization of networks since complex connectivity systems with similar shortest paths distribution can indeed exhibit distinct structures and dynamics. In particular, by neglecting the longer pathways important information is lost about the alternative trails that could connect any two nodes in a network. This information appears strictly related to the concepts of redundancy and robustness, critical resources for the survival of many biological systems as they provide reliable function despite the death of individual elements. Indeed, the presence of more than one path between two nodes in the graph tends to increase the interaction between them, while enhancing the resilience to damages. In particular, the human brain is supposed to exhibit a high level of alternative anatomical and functional pathways between adjacent regions and sites. This type of organization would allow the brain to reshape its physiologic mechanisms in order to compensate the critical consequences of possible diseases (Duffau 2006).

In the present study, we applied the multiple pathways analysis to a dataset of cortical networks that was already studied through standard small-world statistics (De Vico

Fig. 5 Profiles of the permeability index P_h in all the frequency bands. Same conventions as in Fig. 4. Asterisks indicate a significant difference (post-hoc test, $P < 0.01$) between the mean values of the two groups of experimental subjects
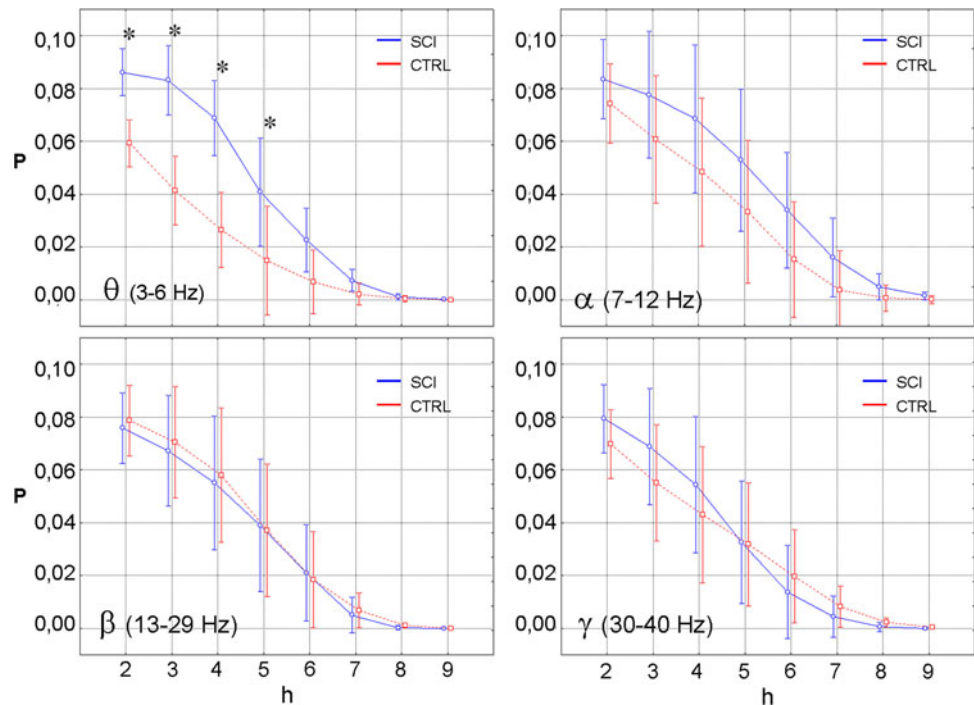

Table 2 Statistical P-values from the ANOVA of the permeability index Ph for each frequency band

Distance *Band*	GROUP	H	GROUP x H
Theta	$F(1,8) = 17.217\ P < 0.001*$	$F(7,56) = 111.96\ P < 0.001*$	$F(7,56) = 9.941\ P < 0.001*$
Alpha	$F(1,8) = 1.83\ P = 0.214$	$F(7,56) = 61.829\ P < 0.001*$	$F(7,56) = 1.006\ P = 0.542$
Beta	$F(1,8) = 0.012\ P = 0.915$	$F(7,56) = 83.624\ P < 0.001*$	$F(7,56) = 0.106\ P = 0.998$
Gamma	$F(1,8) = 0.148\ P = 0.711$	$F(7,56) = 65.508\ P < 0.001*$	$F(7,56) = 1.113\ P = 0.368$

The asterisk symbol * indicates the values $P < 0.01$

Fallani et al. 2007). In that study, interesting differences were observed in the clustering properties of the SCI networks with respect to the CTRL networks in the Theta (3–6 Hz), Alpha (7–12 Hz) and Beta (13–29 Hz) band. In addition, a clear separation from same-sized random networks was found in all the functional connectivity patterns, suggesting a high regular and ordered structure of those brain networks. However, that standard network characterization only took into account shortest paths, while overlooking the remaining longer paths. By following a novel method for the analysis of multiple pathways (Costa and Rodrigues 2008), we defined and we measured the level of redundancy R_h and permeability P_h of those networks by taking into account all the possible paths of length h between node pairs.

The general results indicate that the cortical networks presented different topological properties according to the different distances h, identifying the connectivity ranges. While for R_h values no significant differences came up in any spectral content either between groups or within distances, for P_h values significant ($P < 0.01$) differences

were found in the Theta band (3–6 Hz) between the two groups and within the distances $h = 2, 3, 4$, and 5. This outcome suggests that the overall level of cortical network redundancy is not particularly affected by the spinal trauma that occurred in the SCI patients. In fact, they tend to maintain the same structural connectivity properties of the control subjects by holding a similar average number of alternative paths between *ROIs*. In the opposite way, the network permeability in the SCI brains seems to be more responsive to the indirect effects of the spinal lesion. In particular, the dynamical properties of the SCI networks in the Theta band (3–6 Hz) exhibit a higher significant ($P < 0.01$) tendency to propagate the information flows throughout adjacent ($h < 5$) regions of interests. In other words, the higher permeability indicates that the possible connections tend to form parallel pathways between adjacent nodes or *ROIs*, rather than presenting a general spread of information flow.

Finally, the comparison with a set of random graphs put in evidence the different structural and dynamical properties of the estimated cortical networks. The main effect of
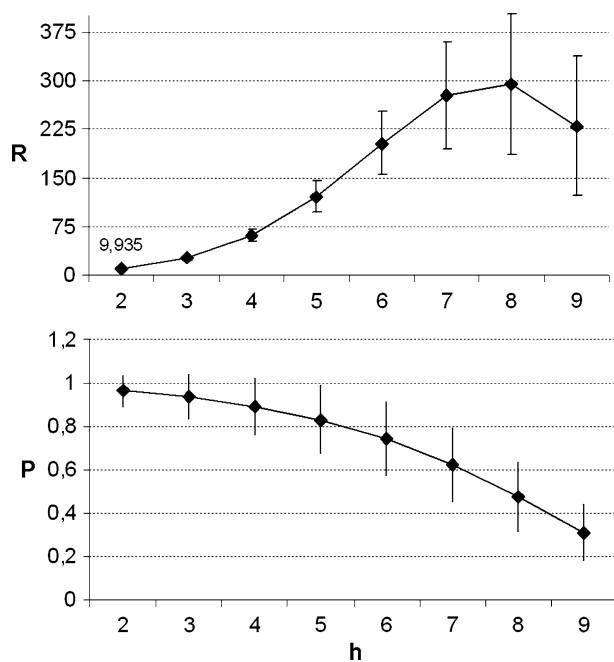
Fig. 6 Profiles of the redundancy index R_h (top) and permeability index P_h (bottom) for random graphs. The different path lengths h are shown on the x-axis. Black circles represent mean values from 100 random graphs with the same number of nodes and links of the original cortical networks. Vertical bars indicate the respective standard deviation

the link shuffling is the formation of a higher number of alternative paths at any distance range (Fig. 6). This effect is a consequence of a lower presence of dead-end nodes, i.e., nodes whose outward number of links is equal to zero. In this way, walks can proceed longer and generate very high values of R_h especially for long distances h. For this reason, random networks exhibit the highest degree of redundancy and permeability. In the present study, both the SCI and CTRL networks presented a significantly lower average number of alternative paths when compared to random graphs, as well as a significantly lower average probability to be connected. This being true at every distance h and in each frequency band (Figs. 4, 5). In particular, the fact that the maximum peak of R_h is located at different distances h for cortical and random networks is a direct consequence of the different organization of the links within the system. In random networks, the probability to find long distance paths is maximal, because in average, everyone is connected with everyone (Strogatz 2001) and one can always find a path, even with a long distance, to connect a node with another one. That is not true in general with real networks, where it is more likely to find non-reachable pairs of nodes because their communication is not possible for physical, anatomical or functional reasons (Boccaletti et al. 2006).

In the light of the results obtained in a previous study (De Vico Fallani et al. 2007), a possible interpretation of

the increased signal propagation observed in the SCI functional network would rely on the need for a higher functional interaction among the closest *ROIs* as a mechanism to compensate the lack of feedback from the peripheral nerves to the sensomotor areas. In particular, the role of the Theta band (3–6 Hz) in these patients could be crucial as it was found significant by two different analyses i.e., the small-world analysis and the multiple pathways analysis reported here. This evidence indicates that the most significant changes in the brain functional network of the SCI patients would occur mainly in the lower spectral contents, which have been already found to be implicated in the preparation of voluntary movements (Popivanov et al. 1999). In particular, these changes are related to an improved propagation of communication between the closest cortical areas rather than to a different degree of redundancy.

Methodological Limitations

The small sample of experimental group ($N = 10$, 5 healthy subjects and 5 patients) represents one limitation that could affect the statistical validity of the results. This limitation is mainly due to the difficulty to find patients participating to the experiment with similar pathological conditions. In order to limit the effects due to this constraint, we adopted the ANOVA statistical method to analyze the obtained results, as it is known to be robust with respect to the departure of normality and homoscedasticity of the data (Zar 1984).

The small number of considered cortical areas (12 *ROIs*) represents another methodological limitation. This limits the power of the theoretical graph approach and restricts the cortical networks to a subset of predefined *ROIs*, which however seem to be the most responsive during this particular experimental task (Mattia et al. 2009). This constraint is related to the procedure to estimate the functional flows between the cortical time series. The Directed Transfer Function (Kaminski et al. 2001) is a powerful method to estimate directed information flows between time series as Granger-causal relationships. However, it needs a large amount of data to compute in a reliable way the connectivity pattern. Given N the number of *ROIs*, O the model order, T the number of EEG time samples and TR the number of trials of the experiment, the following disequation (Kaminski et al. 2001) must be valid:

$$NxNxO < TxTR \tag{5}$$

Meaning that the number of available data points ($TxTR$) must exceed significantly the number of model parameters ($NxNxO$) to be estimated. In our experiment $T = 300$, $TR \sim 100$, $O \sim 10$, $N = 12$ and the number of available data

points is about 20 times the number of parameters, this evidence assuring for reliable functional connectivity patterns.

References

Achard S, Bullmore E (2007) Efficiency and cost of economical brain functional networks. PloS Comput Biol 3(2):e17

Astolfi L, Cincotti F, Mattia D, De Vico Fallani F, Salinari S, Ursino M, Zavaglia M, Marciani MG, Babiloni F (2006) Estimation of the cortical connectivity patterns during the intention of limb movements. IEEE Eng Med Biol Mag 25(4):32–38

Astolfi L, Cincotti F, Mattia D, Marciani MG, Baccalà L, De Vico Fallani F, Salinari S, Ursino M, Zavaglia M, Ding L, Edgar JC, Miller GA, He B, Babiloni F (2007) A comparison of different cortical connectivity estimators for high resolution EEG recordings. Hum Brain Mapp 28(2):143–157

Babiloni F, Babiloni C, Locche L, Cincotti F, Rossini PM, Carducci F (2000) High resolution EEG: source estimates of Laplacian-transformed somatosensory-evoked potentials using a realistic subject head model constructed from magnetic resonance images. Med Biol Eng Comput 38:512–519

Bartolomei F, Bosma I, Klein M, Baayen JC, Reijneveld JC, Postma TJ, Heimans JJ, van Dijk BW, de Munck JC, de Jongh A, Cover KS, Stam CJ (2006) Disturbed functional connectivity in brain tumour patients: evaluation by graph analysis of synchronization matrices. Clin Neurophysiol 117:2039–2049

Bassett DS, Meyer-Linderberg A, Achard S, Th Duke, Bullmore E (2006) Adaptive reconfiguration of fractal smallworld human brain functional networks. Proc Natl Acad Sci USA 103:19518–19523

Boccaletti S, Latora V, Moreno Y, Chavez M, Hwang DU (2006) Complex networks: Structure and dynamics. Phys Rep 424:175–308

Bullmore E, Sporns O (2009) Complex brain networks: graph theoretical analysis of structural and functional systems. Nat Rev Neurosci 10:186–198

Chavez M, Valencia M, Navarro V, Latora V, Martinerie J (2010) Functional modularity of background activities in normal and epileptic brain networks. Phys Rev Lett 104(11):118701

Costa LF, Rodrigues FA. (2008). Superedges: connecting structure and dynamics in complex networks, arXiv:0801.4068v2

De Vico Fallani F, Astolfi L, Cincotti F, Mattia D, Marciani MG, Salinari S, Kurths J, Gao S, Cichocki A, Colosimo A, Babiloni F (2007) Cortical functional connectivity networks in normal and spinal cord injured patients: evaluation by graph analysis. Hum Brain Mapp 28:1334–1336

De Vico Fallani F, Astolfi L, Cincotti F, Mattia D, Marciani MG, Tocci A, Salinari S, Witte H, Hesse W, Gao S, Colosimo A, Babiloni F (2008) Cortical network dynamics during foot movements. Neuroinformatics 6(1):23–34

Duffau H (2006) Brain plasticity: From pathophysiological mechanisms to therapeutic applications. J Clin Neurosci 13:885–897

Eguiluz VM, Chialvo DR, Cecchi GA, Baliki M, Apkarian AV (2005) Scale-free brain functional networks. Phys Rev Lett 94:018102

Gevins A, Le J, Martin N, Brickett P, Desmond J, Reutter B (1994) High resolution EEG: 124-channel recording, spatial deblurring and MRI integration methods. Electroencephalogr Clin Neurophysiol 39:337–358

Goh KI, Kahng B, Kim D (2001) Universal behavior of load distribution in scale-free networks. Phys Rev Lett 87:278701

Granger CWJ (1969) Investigating causal relations by econometric models and cross-spectral methods. Econometrica 37:424–438

Kaminski M, Ding M, Truccolo WA, Bressler S (2001) Evaluating causal relations in neural systems: Granger causality, directed transfer function and statistical assessment of significance. Biol Cybern 85:145–157

Lago-Fernandez LF, Huerta R, Corbacho F, Siguenza JA (2000) Fast response and temporal coherent oscillations in small-world networks, Phys Rev Lett 84:2758–2761

Le J, Gevins A (1993) A method to reduce blur distortion from EEG's using a realistic head model. IEEE Trans Biomed Eng 40:517–528

Maslov S, Sneppen K (2002) Specificity and stability in topology of protein networks. Science 296:910–913

Mattia D, Cincotti F, Astolfi L, De Vico Fallani F, Scivoletto G, Marciani M, Babiloni F (2009) Motor cortical responsiveness to attempted movements in tetraplegia: Evidence from neuroelectrical imaging. Clin Neurophysiol 120(1):181–189

Micheloyannis S, Pachou E, Stam CJ, Vourkas M, Erimaki S, Tsirka V (2006) Using graph theoretical analysis of multi channel EEG to evaluate the neural efficiency hypothesis. Neurosci Lett 402:273–277

Milgram S (1967) The small world problem. Psychol Today 1:60–67

Pfurtsheller G, Lopes da Silva FH (1999) Event-related EEG/EMG synchronizations and desynchronization: basic principles. Clin Neurophysiol 110:1842–1857

Ponten SC, Bartolomei F, Stam CJ (2007) Small-world networks and epilepsy: graph theoretical analysis of intracerebrally recorded mesial temporal lobe seizures. Clin Neurophysiol 118(4):918–927

Popivanov D, Mineva A, Krekule I (1999) EEG patterns in theta and gamma frequency range and their probable relation to human voluntary movement organization. Neurosci Lett 267:5–8

Rodrigues FA, Costa LD (2009) A structure-dynamic approach to cortical organization: Number of paths and accessibility. J Neurosci Methods 183(1):57–62

Rossini PM (2000) Brain redundancy: responsivity or plasticity? Ann Neurol 48(1):128–130

Salvador R, Suckling J, Coleman MR, Pickard JD, Menon D, Bullmore E (2005) Neurophysiological architecture of functional magnetic resonance images of human brain. Cereb Cortex 15(9):1332–1342

Sporns O (2002) Graph theory methods for the analysis of neural connectivity patterns. In: Kötter R (ed) Neuroscience databases A practical guide. Kluwer, Boston, pp 171–186

Sporns O, Tononi G, Edelman GE (2000) Connectivity and complexity: the relationship between neuroanatomy and brain dynamics. Neural Netw 13:909–922

Stam CJ (2004) Functional connectivity patterns of human magnetoencephalographic recordings: a 'small-world' network? Neurosci Lett 355:25–28

Stam CJ, Jones BF, Manshanden I, van Walsum AM, Montez T, Verbunt JP, de Munck JC, van Dijk BW, Berendse HW, Scheltens P (2006) Magnetoencephalographic evaluation of resting-state functional connectivity in Alzheimer's disease. Neuroimage 32:1335–1344

Stam CJ, Jones BF, Nolte G, Breakspear M, Scheltens Ph (2007) Small-world networks and functional connectivity in Alzheimer's disease. Cereb Cortex 17:92–99

Stephan KE, Hilgetag C-C, Burns GAPC, O'Neill MA, Young MP, Kotter R (2000) Computational analysis of functional connectivity between areas of primate cerebral cortex. Phil Trans R Soc Lond B 355:111–126

Strogatz SH (2001) Exploring complex networks. Nature 410:268–276

Tononi G, Sporns O, Edelman GM (1994) A measure for brain complexity: relating functional segregation and integration in the nervous system. Proc Natl Acad Sci USA 91:5033–5037

Watts DJ, Strogatz SH (1998) Collective dynamics of 'small-world' networks. Nature 393:440–442

Zar JH (1984) Biostatistical analysis. Prentice Hall, Englrwood Cliffs